Applied Mathematics Letters 119 (2021) 107181

Contents lists available at ScienceDirect

Applied Mathematics Letters

www.elsevier.com/locate/aml

A novel convergence analysis of Robin–Robin domain decomposition method for Stokes–Darcy system with Beavers–Joseph interface condition

Yingzhi Liu [a], Yinnian He [a], Xuejian Li [b], Xiaoming He [b,*]

[a] *School of Mathematics and Statistics, Xi'an Jiaotong University, Xi'an, 710049, Shaanxi, China*
[b] *Department of Mathematics and Statistics, Missouri University of Science and Technology, Rolla, 65409, MO, USA*

A R T I C L E   I N F O

Article history:
Received 29 December 2020
Received in revised form 2 March 2021
Accepted 2 March 2021
Available online 11 March 2021

Keywords:
Stokes–Darcy system
Domain decomposition method
Robin condition
Convergence analysis

A B S T R A C T

In this paper, we demonstrate the convergence analysis of Robin–Robin domain decomposition method with finite element discretization for Stokes–Darcy system with Beavers-Joseph interface condition, with particular attention paid to the case which is convergent for small viscosity and hydraulic conductivity in practice. Based on the techniques of the discrete harmonic extension and discrete Stokes extension, the convergence is proved and the almost optimal geometric convergence rate is obtained for the case of $\gamma_f > \gamma_p$. Here γ_f and γ_p are positive Robin parameters introduced in Cao et al., 2011, which was not able to show the analysis for $\gamma_f > \gamma_p$ but only numerically illustrated its importance to the convergence for the practical situation with small viscosity and hydraulic conductivity. The analysis result provides a general guideline of choice on the relevant parameters to obtain the convergence and geometric convergence rate. The numerical results verify the theoretical conclusion.

1. Introduction

Stokes–Darcy model couples Stokes equations and Darcy equations with suitable interface conditions. Consider the coupled Stokes–Darcy system on a bounded domain $\Omega = \Omega_D \cup \Omega_S \subset \mathbb{R}^d$, $(d = 2, 3)$, where Ω_D is the porous media domain and Ω_S is the free-flow domain. The free flow in Ω_S can be governed by steady Stokes equations: find the fluid velocity $\boldsymbol{u}_S$ and the kinematic pressure p_S, such that

$$-\nabla \cdot \mathbb{T}(\boldsymbol{u}_S, p_S) = \boldsymbol{f}_S, \quad \nabla \cdot \boldsymbol{u}_S = 0, \quad \text{in } \Omega_S, \tag{1}$$

where $\mathbb{T}(\boldsymbol{u}_S, p_S) = 2\nu\mathbb{D}(\boldsymbol{u}_S) - p_S\mathbb{I}$ is the stress tensor, $\mathbb{D}(\boldsymbol{u}_S) = 1/2(\nabla\boldsymbol{u}_S + \nabla^T\boldsymbol{u}_S)$ is the deformation tensor, ν is the kinematic viscosity of the fluid, and $\boldsymbol{f}_S$ is an given external force. The porous media flow in Ω_D can

* Corresponding author.
E-mail addresses: lyzmath@stu.xjtu.edu.cn (Y. Liu), heyn@xjtu.edu.cn (Y. He), xlcdt@mst.edu (X. Li), hex@mst.edu (X. He).

https://doi.org/10.1016/j.aml.2021.107181

be described by primary Darcy equations: find the hydrostatic pressure ϕ_D, such that

$$-\nabla\cdot(\mathbb{K}\nabla\phi_D)=f_D,\ \text{in}\ \Omega_D, \tag{2}$$

where f_D is a source term and $\mathbb{K}$ is the hydraulic conductivity tensor assumed here to be homogeneous isotropic, i.e. $\mathbb{K}=K\mathbb{I}$ with a constant K. On the interface $\Gamma=\overline{\Omega}_D\cap\overline{\Omega}_S$, the following three interface conditions are imposed:

$$-\boldsymbol{\tau}_j\cdot(\mathbb{T}(\boldsymbol{u}_S,p_S)\cdot\boldsymbol{n}_S)=\alpha\boldsymbol{\tau}_j\cdot(\boldsymbol{u}_S+\mathbb{K}\nabla\phi_D), \tag{3}$$

$$\boldsymbol{u}_S\cdot\boldsymbol{n}_S=\mathbb{K}\nabla\phi_D\cdot\boldsymbol{n}_D,\quad -\boldsymbol{n}_S\cdot(\mathbb{T}(\boldsymbol{u}_S,p_S)\cdot\boldsymbol{n}_S)=g(\phi_D-z), \tag{4}$$

where $\boldsymbol{n}_S$ and $\boldsymbol{n}_D$ denote the unit outer normal to the fluid and the porous media regions on the interface Γ, respectively; $\boldsymbol{\tau}_j$ $(j=1,\ldots,d-1)$ denote mutually orthogonal unit tangential vectors to the interface Γ; α is a constant depending on μ and $\mathbb{K}$. The second condition (3) is the Beavers-Joseph (BJ) interface condition [1–6], which is more difficult than the simplified Beavers–Joseph–Saffman condition [7]. Denote the spaces by

$$X_S=\{\boldsymbol{v}\in[H^1(\Omega_S)]^d\ \mid\ \boldsymbol{v}=0\text{ on }\partial\Omega_S\backslash\Gamma\},\ Q_S=L^2(\Omega_S),\ X_D=\{\psi\in H^1(\Omega_D)\ \mid\ \psi=0\text{ on }\partial\Omega_D\backslash\Gamma\}.$$

For the domain D ($D=\Omega_S$ or Ω_D), $(\cdot,\cdot)_D$ denotes the L^2 inner product on the domain D, and $\langle\cdot,\cdot\rangle$ denotes the L^2 inner product on the interface Γ or the duality pairing between $(H_{00}^{1/2}(\Gamma))'$ and $H_{00}^{1/2}(\Gamma)$. The weak formulation of the coupled system (1)–(4) is to find $(\boldsymbol{u}_S,p_S)\in X_S\times Q_S$ and $\phi_D\in X_D$ such that

$$\begin{aligned}&a_S(\boldsymbol{u}_S,\boldsymbol{v})+b_S(\boldsymbol{v},p_S)+a_D(\phi_D,\psi)+\langle g\phi_D,\boldsymbol{v}\cdot\boldsymbol{n}_S\rangle-\langle\boldsymbol{u}_S\cdot\boldsymbol{n}_S,\psi\rangle+\alpha\langle P_\tau(\boldsymbol{u}_S+\mathbb{K}\nabla\phi_D),P_\tau\boldsymbol{v}\rangle\\&\quad=(f_D,\psi)_{\Omega_D}+(\boldsymbol{f}_S,\boldsymbol{v})_{\Omega_S}+\langle gz,\boldsymbol{v}\cdot\boldsymbol{n}_S\rangle\quad\forall\boldsymbol{v}\in X_S,\ \psi\in X_D,\end{aligned} \tag{5}$$

$$b_S(\boldsymbol{u}_S,q)=0\qquad\forall\,q\in Q_S, \tag{6}$$

where the bilinear forms are defined as

$$a_D(\phi_D,\psi)=(\mathbb{K}\nabla\phi_D,\nabla\psi)_{\Omega_D},\ a_S(\boldsymbol{u}_S,\boldsymbol{v})=2\nu(\mathbb{D}(\boldsymbol{u}_S),\mathbb{D}(\boldsymbol{v}))_{\Omega_S},\ b_S(\boldsymbol{v},q)=-(\nabla\cdot\boldsymbol{v},q)_{\Omega_S},$$

and P_τ denotes the projection onto the tangent space on Γ, i.e. $P_\tau\boldsymbol{u}=\sum_{j=1}^{d-1}(\boldsymbol{u}\cdot\boldsymbol{\tau}_j)\boldsymbol{\tau}_j$.

A parallel Robin–Robin domain decomposition method (DDM) was proposed for the steady Stokes–Darcy model with BJ condition in [8], based on the corresponding basic work for BJS condition [9]. Then this work was extended to steady Naiver–Stokes–Darcy model in [10]. The same Robin–Robin transmission conditions were also utilized to develop a non-iterative domain decomposition method for the unsteady Stokes–Darcy model [11,12]. Based on the Robin conditions for Stokes and Darcy equations

$$\boldsymbol{n}_S\cdot(\mathbb{T}(\boldsymbol{u}_S,p_S)\cdot\boldsymbol{n}_S)+\gamma_f\boldsymbol{u}_S\cdot\boldsymbol{n}_S=\eta_f\ \text{ on }\Gamma,\quad -P_\tau(\mathbb{T}(\boldsymbol{u}_S,p_S)\cdot\boldsymbol{n}_S)-\alpha P_\tau\boldsymbol{u}_S=\boldsymbol{\eta}_{f\tau}\ \text{ on }\Gamma, \tag{7}$$

$$\gamma_p\mathbb{K}\nabla\phi_D\cdot\boldsymbol{n}_D+g\phi_D=\eta_p\ \text{ on }\Gamma, \tag{8}$$

and the compatibility conditions of Lemma 1 in [8], the parallel Robin–Robin DDM was proposed in [8]:

1. Give the initial values $\eta_p^0\in L^2(\Gamma)$, $\eta_f^0\in L^2(\Gamma)$ and $\boldsymbol{\eta}_{f\tau}^0\in\left[L^2(\Gamma)\right]^d$.
2. For $k=0,1,2,\ldots$, independently solve the Stokes and Darcy systems with Robin boundary conditions. More precisely, $\boldsymbol{u}_S^k\in X_S$ and $p_S^k\in Q_S$ are computed from

$$\begin{aligned}&a_S(\boldsymbol{u}_S^k,\boldsymbol{v})+b_S(\boldsymbol{v},p_S^k)+\gamma_f\langle\boldsymbol{u}_S^k\cdot\boldsymbol{n}_S,\boldsymbol{v}\cdot\boldsymbol{n}_S\rangle+\alpha\langle P_\tau\boldsymbol{u}_S^k,P_\tau\boldsymbol{v}\rangle\\&\quad=\langle\eta_f^k,\boldsymbol{v}\cdot\boldsymbol{n}_S\rangle-\langle\boldsymbol{\eta}_{f\tau}^k,P_\tau\boldsymbol{v}\rangle+(\boldsymbol{f}_S,\boldsymbol{v})_{\Omega_S}\quad\forall\,\boldsymbol{v}\in X_S,\end{aligned} \tag{9}$$

$$b_S(\boldsymbol{u}_S^k,q)=0\quad\forall\,q\in Q_S, \tag{10}$$

and $\phi_D^k\in X_D$ is computed from

$$a_D(\phi_D^k,\psi)+\langle\frac{g\phi_D^k}{\gamma_p},\psi\rangle=\langle\frac{\eta_p^k}{\gamma_p},\psi\rangle+(f_D,\psi)_{\Omega_D}\qquad\forall\,\psi\in X_D. \tag{11}$$

3. Update η_p^{k+1} and η_f^{k+1}:

$$\eta_f^{k+1} = \frac{\gamma_f}{\gamma_p}\eta_p^k - (1+a)g\phi_D^k + gz,\ \boldsymbol{\eta}_{f\tau}^{k+1} = \alpha P_\tau(\mathbb{K}\nabla\phi_D^k),\ \eta_p^{k+1} = -\eta_f^k + (\gamma_f+\gamma_p)\boldsymbol{u}_S^k\cdot\boldsymbol{n}_S + gz. \quad (12)$$

In [8,10] the convergence of Robin–Robin DDM was proved for $\gamma_f \le \gamma_p$, and the geometric convergence rate $(\gamma_f\gamma_p^{-1})^{1/2}$ was obtained when $\gamma_f < \gamma_p$. This result works well for the case with moderate viscosity ν and hydraulic conductivity K. However, for most of the practical coefficients, such as $\nu = 10^{-6}$ and $10^{-7} \le K \le 10^{-2}$ which may cause severe computational difficulties [13], the Robin–Robin DDM with finite element discretization seems difficult to converge for $\gamma_f < \gamma_p$ according to the results in [8]. Although the numerical experiments in [8] indicate that Robin parameter $\gamma_f > \gamma_p$ might provide decent convergence results for small ν and K, there was not a complete analysis to support their observations due to the difficulty arising from the coupling feature of the model, especially the Beavers-Joseph interface condition. Motivated by the practical applications and analysis difficulty, we provide a rigorous analysis with novel techniques based on the discrete harmonic extension and discrete Stokes extension to prove the convergence and the geometric convergence rate of Robin–Robin algorithm when $\gamma_f > \gamma_p$.

2. Convergence analysis for the finite element discretization of the proposed DDM

In this section, we consider the regular triangulation $\mathcal{T}_h$ with uniform mesh size h for the domain Ω_D and Ω_S. $\mathcal{T}_h$ is assumed to be shape-regular and quasi-uniform as well. The Taylor–Hood finite element pair and the quadratic finite elements are considered for the Stokes equations and the primary formulation of the Darcy equations, respectively. The finite element spaces for the coupled Stokes–Darcy problem (1)–(4) are denoted as $X_{Sh} \in X_S$, $Q_{Sh} \in Q_S$, and $X_{Dh} \in X_D$. Then the finite element solution space of the decoupled Stokes–Darcy system (5)–(6) and (9)–(11) are given $\phi_{Dh}, \phi_{Dh}^k \in X_{Dh}$, $\boldsymbol{u}_{Sh}, \boldsymbol{u}_{Sh}^k \in X_{Sh}$, and $p_{Sh}, p_{Sh}^k \in Q_{Sh}$. Due to the page limitation, we omit the details of the discrete weak formulations which can be obtained from (5)–(6) and (9)–(11) by adding h in the subscript of all the unknown functions and test functions. Then, we define the error functions

$$e_\phi^k = \phi_{Dh} - \phi_{Dh}^k,\ \boldsymbol{e}_u^k = \boldsymbol{u}_{Sh} - \boldsymbol{u}_{Sh}^k,\ e_p^k = p_{Sh} - p_{Sh}^k,\ \varepsilon_D^k = \eta_{ph} - \eta_{ph}^k,\ \varepsilon_S^k = \eta_{fh} - \eta_{fh}^k,\ \boldsymbol{\varepsilon}_{S\tau}^k = \boldsymbol{\eta}_{f\tau h} - \boldsymbol{\eta}_{f\tau h}^k,$$

and derive the error equations

$$\gamma_p a_D(e_\phi^k, \psi_h) + \langle g e_\phi^k, \psi_h\rangle = \langle \varepsilon_D^k, \psi_h\rangle \quad \forall\, \psi_h \in X_{Dh}, \quad (13)$$

$$a_S(\boldsymbol{e}_u^k, \boldsymbol{v}) + b_S(\boldsymbol{v}, e_p^k) + \gamma_f\langle \boldsymbol{e}_u^k\cdot\boldsymbol{n}_S, \boldsymbol{v}\cdot\boldsymbol{n}_S\rangle + \alpha\langle P_\tau\boldsymbol{e}_u^k, P_\tau\boldsymbol{v}\rangle = \langle \varepsilon_S^k, \boldsymbol{v}\cdot\boldsymbol{n}_S\rangle - \langle \boldsymbol{\varepsilon}_{S_\tau}^k, P_\tau\boldsymbol{v}_h\rangle \quad \forall\, \boldsymbol{v}_h \in X_{Sh}, \quad (14)$$

$$b_S(\boldsymbol{e}_u^k, q_h) = 0 \quad \forall\, q_h \in Q_{Sh}, \quad (15)$$

based on (5)–(6), (9)–(11) and their finite element discretization formulations. Similar to Lemma 2 in [8], we can obtain the following lemma.

Lemma 2.1. *The error functions satisfy*

$$\|\varepsilon_D^{k+1}\|_\Gamma^2 = \|\varepsilon_S^k\|_\Gamma^2 + (\gamma_p^2 - \gamma_f^2)\|\boldsymbol{e}_u^k\cdot\boldsymbol{n}_S\|_\Gamma^2 - 2(\gamma_f+\gamma_p)a_s(\boldsymbol{e}_u^k, \boldsymbol{e}_u^k) - 2(\gamma_f+\gamma_p)\alpha\langle P_\tau(\boldsymbol{e}_u^k + \mathbb{K}\nabla e_\phi^{k-1}), P_\tau\boldsymbol{e}_u^k\rangle, \quad (16)$$

$$\|\varepsilon_S^{k+1}\|_\Gamma^2 = \left(\frac{\gamma_f}{\gamma_p}\right)^2\|\varepsilon_D^k\|_\Gamma^2 + \left(1 - \left(\frac{\gamma_f}{\gamma_p}\right)^2\right)\|g e_\phi^k\|_\Gamma^2 - 2\gamma_f\left(1 + \frac{\gamma_f}{\gamma_p}\right) g a_D(e_\phi^k, e_\phi^k). \quad (17)$$

In (16) and (17), the two terms involving $\|\boldsymbol{e}_u^k \cdot \boldsymbol{n}_S\|_\Gamma^2$ and $\|ge_\phi^k\|_\Gamma^2$ are negative when $\gamma_f > \gamma_p$, which is one of the main problems encountered in the original analysis framework [8]. To address such difficulty and continue the convergence analysis, we introduce key estimates for ε_D and ε_S by employing discrete harmonic extension, discrete Stokes extension and the inverse inequality [14].

Lemma 2.2. *Let $\Omega \subset \mathbb{R}^d$ and $V_h(\Omega) \subset H^1(\Omega)$ be the finite element space with shape-regular and quasi-uniform triangulation $\mathcal{T}_h$. Then for any $u_h \in V_h(\Omega)$, we have*

$$|u_h|_{H^{1/2},\partial\Omega} \le Ch^{-1/2}\|u_h\|_{0,\partial\Omega}. \tag{18}$$

Lemma 2.3. *Assume that $K < \gamma_p^{-1}h$ and $\nu < h$. Then ε_D^k satisfies*

$$\|\varepsilon_D^k\|_\Gamma^2 \le \frac{1}{1-K\gamma_p h^{-1}}\gamma_p a_D(e_\phi^k, e_\phi^k) + \frac{1}{1-K\gamma_p h^{-1}}\|ge_\phi^k\|_\Gamma^2. \tag{19}$$

ε_S^k satisfies

$$\|\varepsilon_S^k\|_\Gamma^2 \le \frac{1}{1-\nu h^{-1}}\left(a_S(\boldsymbol{e}_u^k, \boldsymbol{e}_u^k) + \gamma_f^2\|\boldsymbol{e}_u^k \cdot \boldsymbol{n}_S\|_\Gamma^2\right). \tag{20}$$

Proof. Let $E\varepsilon_D^k \in X_{Dh}$ be the discrete harmonic extension of ε_D^k [14,15], i.e., $E\varepsilon_D^k = \varepsilon_D^k$ on Γ and satisfy

$$(\nabla E\varepsilon_D^k, \nabla\psi_h)_{\Omega_D} = 0, \quad \forall \psi_h \in X_{Dh}^0 := X_{Dh} \cap H_0^1(\Omega_D). \tag{21}$$

Then the discrete harmonic extension $E\varepsilon_D^k$ satisfies (see Lemma 4.10 in [14])

$$|\varepsilon_D^k|^2_{H_{00}^{1/2},\Gamma} \approx |E\varepsilon_D^k|^2_{H^{1/2},\partial\Omega_D} \approx |E\varepsilon_D^k|_1^2. \tag{22}$$

Setting $\psi_h = E\varepsilon_D^k$ and substituting into (13), we have

$$\langle \varepsilon_D^k, \varepsilon_D^k\rangle = \gamma_p a_D(e_\phi^k, E\varepsilon_D^k) + \langle ge_\phi^k, \varepsilon_D^k\rangle. \tag{23}$$

Hence, using Cauchy–Schwarz inequality, (22) and (18), we can obtain from (23) that

$$\begin{aligned}\|\varepsilon_D^k\|_\Gamma^2 &\le \gamma_p a_D(e_\phi^k, e_\phi^k)^{\frac12} a_D(E\varepsilon_D^k, E\varepsilon_D^k)^{\frac12} + \|ge_\phi^k\|_\Gamma\|\varepsilon_D^k\|_\Gamma \\ &\le \gamma_p a_D(e_\phi^k, e_\phi^k)^{\frac12} K^{\frac12} h^{-1/2}\|\varepsilon_D^k\|_\Gamma + \|ge_\phi^k\|_\Gamma\|\varepsilon_D^k\|_\Gamma \\ &\le 1/2\gamma_p a_D(e_\phi^k, e_\phi^k) + 1/2K\gamma_p h^{-1}\|\varepsilon_D^k\|_\Gamma^2 + 1/2\|ge_\phi^k\|_\Gamma^2 + 1/2\|\varepsilon_D^k\|_\Gamma^2,\end{aligned} \tag{24}$$

which completes the proof of (19).

Similarly, let $\boldsymbol{E}\varepsilon_S^k \in X_{Sh}$ be the discrete Stokes extension of ε_S^k [14,16,17], i.e., $\boldsymbol{E}\varepsilon_S^k = \varepsilon_S^k\boldsymbol{n}_S$ and satisfy

$$a_S(\boldsymbol{E}\varepsilon_S^k, \boldsymbol{v}_h) + b_S(\boldsymbol{E}\varepsilon_S^k, q_h) + b_S(\boldsymbol{v}_h, p_S) = 0 \quad \forall \boldsymbol{v}_h \in X_{Sh}^0,\ q_h \in Q_{Sh}, \tag{25}$$

with $p_S \in Q_{Sh}^0$. Here $X_{Sh}^0 := X_{Sh} \cap [H_0^1(\Omega_S)]^d$, $Q_{Sh}^0 := Q_{Sh} \cap L_0^2(\Omega_S)$ and $L_0^2(\Omega_S) = \left\{q \in L^2(\Omega_S) : \int_{\Omega_S} q = 0\right\}$. Then the solution $\boldsymbol{E}\varepsilon_S^k$ of (25) satisfies (see Lemma 9.10 in [14])

$$|\varepsilon_S^k|^2_{H_{00}^{1/2},\Gamma} \approx |\boldsymbol{E}\varepsilon_S^k|^2_{H^{1/2},\partial\Omega_S} \approx |\boldsymbol{E}\varepsilon_S^k|_1^2,\ P_\tau\boldsymbol{E}\varepsilon_S^k = 0,\ b_S(\boldsymbol{E}\varepsilon_S^k, q_h) = 0 \quad \forall q_h \in Q_{Sh}. \tag{26}$$

Setting $\psi_h = \boldsymbol{E}\varepsilon_S^k$ and substituting into (14)–(15), we have

$$\langle \varepsilon_S^k, \varepsilon_S^k\rangle = a_S(\boldsymbol{e}_u^k, \boldsymbol{E}\varepsilon_S^k) + \gamma_f\langle \boldsymbol{e}_u^k \cdot \boldsymbol{n}_S, \varepsilon_S^k\rangle. \tag{27}$$

Therefore, using Cauchy–Schwarz inequality, (26) and (18), we can find from (27) that

$$\begin{aligned} \|\varepsilon_S^k\|_\Gamma^2 &= a_S(\boldsymbol{e}_u^k, \boldsymbol{E}\varepsilon_S^k) + \gamma_f \langle \boldsymbol{e}_u^k \cdot \boldsymbol{n}_S, \varepsilon_S^k \rangle \\ &\le a_S(\boldsymbol{e}_u^k, \boldsymbol{e}_u^k)^{1/2} a_S(\boldsymbol{E}\varepsilon_S^k, \boldsymbol{E}\varepsilon_S^k)^{1/2} + \gamma_f \|\boldsymbol{e}_u^k \cdot \boldsymbol{n}_S\|_\Gamma \|\varepsilon_S^k\|_\Gamma \\ &\le 1/2 a_S(\boldsymbol{e}_u^k, \boldsymbol{e}_u^k) + 1/2\nu |\varepsilon_S^k|^2_{H_{00}^{1/2},\Gamma} + 1/2\gamma_f^2 \|\boldsymbol{e}_u^k \cdot \boldsymbol{n}_S\|_\Gamma^2 + 1/2 \|\varepsilon_S^k\|_\Gamma^2 \\ &\le 1/2 a_S(\boldsymbol{e}_u^k, \boldsymbol{e}_u^k) + 1/2\gamma_f^2 \|\boldsymbol{e}_u^k \cdot \boldsymbol{n}_S\|_\Gamma^2 + 1/2(1+\nu h^{-1}) \|\varepsilon_S^k\|_\Gamma^2, \end{aligned} \tag{28}$$

which leads to (20). □

Following the inequalities (5.35)–(5.36) in [8], when α is small enough, we can similarly obtain

$$\begin{aligned} &\sum_{k=1}^{N} \left(a_s(\boldsymbol{e}_u^k, \boldsymbol{e}_u^k) + \alpha \langle P_\tau(\boldsymbol{e}_u^k + \mathbb{K}\nabla e_\phi^{k-1}), P_\tau \boldsymbol{e}_u^k \rangle + g a_D(e_\phi^k, e_\phi^k) \right) \\ &\ge (C_1(K,v) - C_2(K)\alpha) \sum_{k=0}^{N} \left(\|\boldsymbol{e}_u^k\|_1^2 + \|e_\phi^k\|_1^2 \right) - C_1(K,v) \left(\|\boldsymbol{e}_u^0\|_1^2 + \|e_\phi^0\|_1^2 \right), \end{aligned} \tag{29}$$

where C_1 depends on K and ν linearly and C_2 depends on K linearly.

Now we present the convergence results of the Robin–Robin algorithm for $\gamma_f > \gamma_p$.

Theorem 2.1. *Assume that $K < \gamma_p^{-1} h$, $\nu < h$, and α is small enough such that $C_1(K,\nu) - C_2(K)\alpha > 0$. C_i $(i = 1, \dots, 5)$ are constants which depend on K and ν linearly. For $\gamma_f > \gamma_p$, the Robin–Robin algorithm converges in the discrete sense if γ_f and γ_p satisfy*

$$\frac{\gamma_f}{\gamma_p} \ge 1 + 2\delta K \gamma_p h^{-1}, \ \frac{\gamma_f}{\gamma_p} \le \frac{h}{\beta \gamma_f K}, \ \frac{\gamma_f}{\gamma_p} \le 1 + \frac{h}{\nu} \frac{C_1(K,\nu) - C_2(K)\alpha}{\beta K}, \tag{30}$$

where $\delta = \left(\frac{\gamma_f}{\gamma_p}\right)^2 - 1$ and $\beta = (1 - \nu h^{-1})^{-1} > 1$. Further assume that γ_f and γ_p satisfy

$$\theta \ge 1 - \frac{(\gamma_f + \gamma_p) C_4(K,\nu)}{\beta \nu}, \ \theta \ge \frac{2\alpha \gamma_p C_3(K)}{(\gamma_f + \gamma_p) C_5(K)}, \tag{31}$$

where $\theta = (1+\epsilon)\left(\frac{\gamma_p}{\gamma_f}\right)^2$ and $\epsilon = \delta \nu h^{-1}$. Then the geometric convergence rate $\sqrt{\frac{\gamma_p}{\gamma_f}} \left(1 + O(Kh^{-1} + \nu h^{-1})\right)$ is obtained.

Proof. Let δ_2 be a positive constant. Multiplying (16) by δ_2 and adding into (17), then summing over k from $k = 1$ to N and using the fact $-2\gamma_f \left(1 + \frac{\gamma_f}{\gamma_p}\right) = -2\delta_2 (\gamma_f + \gamma_p) - 2(\gamma_f + \gamma_p)\left(\frac{\gamma_f}{\gamma_p} - \delta_2\right)$, we deduce

$$\begin{aligned} &\delta_2 \|\varepsilon_D^{N+1}\|_\Gamma^2 + \|\varepsilon_S^{N+1}\|_\Gamma^2 \le \delta_2 \|\varepsilon_D^1\|_\Gamma^2 + \|\varepsilon_S^1\|_\Gamma^2 + \left(\left(\frac{\gamma_f}{\gamma_p}\right)^2 - \delta_2\right) \sum_{k=1}^{N} \|\varepsilon_D^k\|_\Gamma^2 + (\delta_2 - 1) \sum_{k=1}^{N} \|\varepsilon_S^k\|_\Gamma^2 \\ &- \left(\left(\frac{\gamma_f}{\gamma_p}\right)^2 - 1\right) \sum_{k=1}^{N} \|g e_\phi^k\|_\Gamma^2 + \delta_2 \left(\gamma_p^2 - \gamma_f^2\right) \sum_{k=1}^{N} \|\boldsymbol{e}_u^k \cdot \boldsymbol{n}_S\|_\Gamma^2 - 2(\gamma_f + \gamma_p)\left(\frac{\gamma_f}{\gamma_p} - \delta_2\right) g \sum_{k=1}^{N} a_D(e_\phi^k, e_\phi^k) \\ &- 2\delta_2 (\gamma_f + \gamma_p) \sum_{k=1}^{N} \left(a_s(\boldsymbol{e}_u^k, \boldsymbol{e}_u^k) + \alpha \langle P_\tau(\boldsymbol{e}_u^k + \mathbb{K}\nabla e_\phi^{k-1}), P_\tau \boldsymbol{e}_u^k \rangle + g a_D(e_\phi^k, e_\phi^k) \right). \end{aligned} \tag{32}$$

Using (29), we obtain from (32) that

$$\delta_2\|\varepsilon_D^{N+1}\|_\Gamma^2+\|\varepsilon_S^{N+1}\|_\Gamma^2\le\delta_2\|\varepsilon_D^1\|_\Gamma^2+\|\varepsilon_S^1\|_\Gamma^2+\left(\left(\frac{\gamma_f}{\gamma_p}\right)^2-\delta_2\right)\sum_{k=1}^N\|\varepsilon_D^k\|_\Gamma^2+(\delta_2-1)\sum_{k=1}^N\|\varepsilon_S^k\|_\Gamma^2$$
$$-\left(\left(\frac{\gamma_f}{\gamma_p}\right)^2-1\right)\sum_{k=1}^N\|ge_\phi^k\|_\Gamma^2-\delta_2\left(\gamma_f^2-\gamma_p^2\right)\sum_{k=1}^N\|\boldsymbol{e}_u^k\cdot\boldsymbol{n}_S\|_\Gamma^2-2\left(\gamma_f+\gamma_p\right)\left(\frac{\gamma_f}{\gamma_p}-\delta_2\right)g\sum_{k=1}^N a_D(e_\phi^k,e_\phi^k)$$
$$-2\delta_2\left(\gamma_f+\gamma_p\right)\left(C_1(K,v)-C_2(K)\alpha\right)\sum_{k=1}^N\left(\|\boldsymbol{e}_u^k\|_1^2+\|e_\phi^k\|_1^2\right)+2\delta_2C_1(K,v)\left(\gamma_f+\gamma_p\right)\left(\|\boldsymbol{e}_u^0\|_1^2+\|e_\phi^0\|_1^2\right).\quad(33)$$

Denote $\delta_1=(1-K\gamma_ph^{-1})^{-1}$ and restrict $\left(\frac{\gamma_f}{\gamma_p}\right)^2-\delta_2>0$. Then from Lemma 2.3, we have

$$\left(\left(\frac{\gamma_f}{\gamma_p}\right)^2-\delta_2\right)\|\varepsilon_D^k\|_\Gamma^2\le\left(\left(\frac{\gamma_f}{\gamma_p}\right)^2-\delta_2\right)\delta_1\gamma_pa_D(e_\phi^k,e_\phi^k)+\left(\left(\frac{\gamma_f}{\gamma_p}\right)^2-\delta_2\right)\delta_1\|ge_\phi^k\|_\Gamma^2.\quad(34)$$

Set $\delta=\left(\frac{\gamma_f}{\gamma_p}\right)^2-1$ and then choose δ_2 by satisfying the following inequality

$$0<\left(\left(\frac{\gamma_f}{\gamma_p}\right)^2-\delta_2\right)\delta_1\le\delta,\quad\text{i.e. }1+\delta K\gamma_ph^{-1}\le\delta_2<\left(\frac{\gamma_f}{\gamma_p}\right)^2.\quad(35)$$

Substituting (34) and (35) into (33), we obtain

$$\delta_2\|\varepsilon_D^{N+1}\|_\Gamma^2+\|\varepsilon_S^{N+1}\|_\Gamma^2\le\delta_2\|\varepsilon_D^1\|_\Gamma^2+\|\varepsilon_S^1\|_\Gamma^2+2\delta_2C_1(K,v)\left(\gamma_f+\gamma_p\right)\left(\|\boldsymbol{e}_u^0\|_1^2+\|e_\phi^0\|_1^2\right)$$
$$+\left(\gamma_p\delta-2\left(\gamma_f+\gamma_p\right)\left(\frac{\gamma_f}{\gamma_p}-\delta_2\right)g\right)\sum_{k=1}^N a_D(e_\phi^k,e_\phi^k)-\delta_2\left(\gamma_f^2-\gamma_p^2\right)\sum_{k=1}^N\|\boldsymbol{e}_u^k\cdot\boldsymbol{n}_S\|_\Gamma^2$$
$$+(\delta_2-1)\sum_{k=1}^N\|\varepsilon_S^k\|_\Gamma^2-2\delta_2\left(\gamma_f+\gamma_p\right)\left(C_1(K,v)-C_2(K)\alpha\right)\sum_{k=1}^N\left(\|\boldsymbol{e}_u^k\|_1^2+\|e_\phi^k\|_1^2\right).\quad(36)$$

Using Lemma 2.3 and setting $\beta=(1-\nu h^{-1})^{-1}>1$ (when $h>\nu>0$), we find that

$$(\delta_2-1)\|\varepsilon_S^k\|_\Gamma^2\le2\nu\beta(\delta_2-1)\|\boldsymbol{e}_u^k\|_1^2+\gamma_f^2\beta(\delta_2-1)\|\boldsymbol{e}_u^k\cdot\boldsymbol{n}_S\|_\Gamma^2.\quad(37)$$

Substituting (37) into (36) and re-arranging the terms on the two sides, we have

$$\left(2\left(\gamma_f+\gamma_p\right)\left(\frac{\gamma_f}{\gamma_p}-\delta_2\right)g-\gamma_p\delta\right)\sum_{k=1}^N a_D(e_\phi^k,e_\phi^k)+\left(\delta_2\left(\gamma_f^2-\gamma_p^2\right)-\gamma_f^2\beta(\delta_2-1)\right)\sum_{k=1}^N\|\boldsymbol{e}_u^k\cdot\boldsymbol{n}_S\|_\Gamma^2$$
$$+\ \left(2\delta_2\left(\gamma_f+\gamma_p\right)\left(C_1(K,v)-C_2(K)\alpha\right)-2\nu\beta(\delta_2-1)\right)\sum_{k=1}^N\left(\|\boldsymbol{e}_u^k\|_1^2+\|e_\phi^k\|_1^2\right)+\delta_2\|\varepsilon_D^{N+1}\|_\Gamma^2+\|\varepsilon_S^{N+1}\|_\Gamma^2$$
$$\le\delta_2\|\varepsilon_D^1\|_\Gamma^2+\|\varepsilon_S^1\|_\Gamma^2+2\delta_2C_1(K,v)\left(\gamma_f+\gamma_p\right)\left(\|\boldsymbol{e}_u^0\|_1^2+\|e_\phi^0\|_1^2\right).\quad(38)$$

Now taking $\delta_2=1+\delta K\gamma_ph^{-1}$ and setting $g=1$, we consider the following three cases:

- Suppose $A_1:=2\left(\gamma_f+\gamma_p\right)\left(\frac{\gamma_f}{\gamma_p}-\delta_2\right)g-\gamma_p\delta\ge0$. Then we get $\delta_2\le\frac{1}{2}\left(1+\frac{\gamma_f}{\gamma_p}\right)$ for the first condition in (30).
- Suppose $A_2:=\delta_2\left(\gamma_f^2-\gamma_p^2\right)-\gamma_f^2\beta(\delta_2-1)\ge0$. Then from $A_2>\left(\gamma_f^2-\gamma_p^2\right)\left(1-\gamma_f^2\gamma_p^{-1}\beta Kh^{-1}\right)\ge0$, we have the second condition in (30).

- Suppose $A_3 := 2\delta_2(\gamma_f+\gamma_p)(C_1(K,v)-C_2(K)\alpha) - 2\nu\beta(\delta_2-1) \geq 0$. Then using $C_1(K,v)-C_2(K)\alpha > 0$ and $A_3 > 2(\gamma_f+\gamma_p)\left((C_1(K,v)-C_2(K)\alpha) - \beta\left(\frac{\gamma_f}{\gamma_p}-1\right)\nu K h^{-1}\right) \geq 0$, we have $\frac{\gamma_p}{\gamma_f-\gamma_p} \geq \frac{\beta h^{-1}\nu K}{C_1(K,v)-C_2(K)\alpha}$, which means the third condition in (30).

Since the right hand side of (38) is uniformly bounded for arbitrary N, then $\sum_{k=1}^{N}\left(\|\boldsymbol{e}_u^k\|_1^2 + \|e_\phi^k\|_1^2\right)$ is upper bounded for arbitrary N based on the assumptions of Theorem 2.1. Hence $\|\boldsymbol{e}_u^k\|_1$ and $\|e_\phi^k\|_1$ go to 0 when N goes to infinity, which provides the convergence of $\boldsymbol{u}_{Sh}^k$ and ϕ_{Dh}^k.

Now we turn to the proof of the almost geometric convergence rate. Based on the inequality (29), the coercivity of a_S and the trace theorems [18], for small α, we can find that

$$\begin{aligned} &a_S(\boldsymbol{e}_u^k,\boldsymbol{e}_u^k) + \alpha\langle P_\tau(\boldsymbol{e}_u^k + \mathbb{K}\nabla e_\phi^{k-1}), P_\tau \boldsymbol{e}_u^k\rangle \geq a_S(\boldsymbol{e}_u^k,\boldsymbol{e}_u^k) + \alpha\|P_\tau \boldsymbol{e}_u^k\|_\Gamma^2 - \alpha\|\mathbb{K}\nabla e_\phi^{k-1}\|_{-1/2,\Gamma}\|P_\tau\boldsymbol{e}_u^k\|_{1/2,\Gamma} \\ &\geq a_S(\boldsymbol{e}_u^k,\boldsymbol{e}_u^k) - \alpha C_3(K)\left(\|e_\phi^{k-1}\|_1^2 + \|\boldsymbol{e}_u^k\|_1^2\right) \geq C_4(K,v)\|\boldsymbol{e}_u^k\|_1^2 - \alpha C_3(K)\|e_\phi^{k-1}\|_1^2, \end{aligned} \tag{39}$$

where C_3 depends on K linearly and C_4 depends on K and ν linearly. By the coercivity of a_D, we have

$$a_D(e_\phi^k, e_\phi^k) \geq C_5(K)\|e_\phi^k\|_1^2, \tag{40}$$

where C_5 depends on K linearly. Then splitting $\|\varepsilon_S^k\|_\Gamma^2 = \theta\|\varepsilon_S^k\|_\Gamma^2 + (1-\theta)\|\varepsilon_S^k\|_\Gamma^2$ with $0\leq\theta\leq 1$, substituting (17) into (16) and using (19), (20), (39) and (40), we have

$$\begin{aligned} \|\varepsilon_D^{k+1}\|_\Gamma^2 = {} & \theta\delta_2\|\varepsilon_D^{k-1}\|_\Gamma^2 + \theta\left(\left(\frac{\gamma_f}{\gamma_p}\right)^2 - \delta_2\right)\|\varepsilon_D^{k-1}\|_\Gamma^2 + \theta\left(1-\left(\frac{\gamma_f}{\gamma_p}\right)^2\right)\|g e_\phi^{k-1}\|_\Gamma^2 \\ & - 2\theta\gamma_f\left(1+\frac{\gamma_f}{\gamma_p}\right) g a_D(e_\phi^{k-1}, e_\phi^{k-1}) \\ & + (1-\theta)\|\varepsilon_S^k\|_\Gamma^2 + (\gamma_p^2-\gamma_f^2)\|\boldsymbol{e}_u^k\cdot\boldsymbol{n}_S\|_\Gamma^2 - 2(\gamma_f+\gamma_p)a_s(\boldsymbol{e}_u^k,\boldsymbol{e}_u^k) \\ & - 2(\gamma_f+\gamma_p)\alpha\langle P_\tau(\boldsymbol{e}_u^k+\mathbb{K}\nabla e_\phi^{k-1}), P_\tau\boldsymbol{e}_u^k\rangle. \\ \leq {} & \theta\delta_2\|\varepsilon_D^{k-1}\|_\Gamma^2 - \left((\gamma_f^2-\gamma_p^2) - (1-\theta)\gamma_f^2\beta\right)\|\boldsymbol{e}_u^k\cdot\boldsymbol{n}_S\|_\Gamma^2 - \left(2(\gamma_f+\gamma_p)C_4(K,\nu) - 2(1-\theta)\nu\beta\right)\|\boldsymbol{e}_u^k\|_1^2 \\ & - \left(2\theta(\gamma_f+\gamma_p)\frac{\gamma_f}{\gamma_p}g - \theta\gamma_p\delta\right)C_5(K)\|e_\phi^{k-1}\|_1^2 + 2(\gamma_f+\gamma_p)\alpha C_3(K)\|e_\phi^{k-1}\|_1^2. \end{aligned} \tag{41}$$

Setting $\theta = (1+\epsilon)\left(\frac{\gamma_p}{\gamma_f}\right)^2$ and $g=1$, we consider the following assumptions

- Suppose $B_1 := \left(\gamma_f^2-\gamma_p^2\right) - (1-\theta)\gamma_f^2\beta \geq 0$. Then we find $\epsilon \geq \left(\left(\frac{\gamma_f}{\gamma_p}\right)^2 - 1\right)\frac{\beta-1}{\beta} = \delta\nu h^{-1}$.
- Suppose $B_2 := 2(\gamma_f+\gamma_p)C_4(K,\nu) - 2(1-\theta)\nu\beta \geq 0$. Then we have the first condition in (31).
- Suppose $B_3 := \left(2\theta(\gamma_f+\gamma_p)\frac{\gamma_f}{\gamma_p}g - \theta\gamma_p\delta\right)C_5(K) - 2(\gamma_f+\gamma_p)\alpha C_3(K) \geq 0$. Then we obtain the second condition in (31).

Now choose $\epsilon = \delta\nu h^{-1}$ and then for small K and ν we can see that the setting $\theta = (1+\epsilon)\left(\frac{\gamma_p}{\gamma_f}\right)^2$ holds for the above assumptions of B_1, B_2 and B_3. Finally, from (41), we achieve the almost optimal geometric convergence rate $\rho = (\theta\delta_2)^{1/4} = \sqrt{\frac{\gamma_p}{\gamma_f}}\left((1+\delta K\gamma_p h^{-1})(1+\delta\nu h^{-1})\right)^{1/4} = \sqrt{\frac{\gamma_p}{\gamma_f}}\left(1+O(Kh^{-1}+\nu h^{-1})\right)$. □

Remark 2.1. From the above proof, we can see that C_1 and C_4 depend on K and ν linearly while C_2, C_3, and C_5 depend on K linearly. The coefficients of K and ν in these linear relationships come from the involved inequalities in the corresponding proof and are usually bounded (not too big or too small) for regular cases. For example, one can simply take $C_5 = K$ and $C_2 = C_3 = cK$ where c is a constant coming from the upper bound of the trace inequality. These regular linear relationships together with the other regular parameters are helpful for finding appropriate γ_f and γ_p based on the conditions in Theorem 2.1.

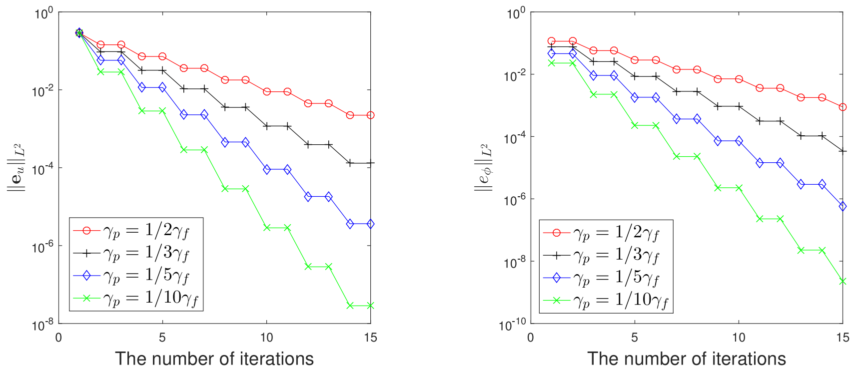

Fig. 1. L^2 errors in velocity (left) and hydraulic head (right) versus the number of iterations for the parallel Robin–Robin domain decomposition method with $\gamma_f > \gamma_p$.

Remark 2.2. In the international parameter system, the real-life parameters K and ν are usually very small [19]. In this case, the right hand side of the first inequality in (30) is not big and the right hand sides of the last two inequalities in (30) are not small, if other constants and parameters in (30) are regular. Therefore, it is not hard to find γ_f and γ_p, which cannot be too big, to satisfy the three inequalities in (30). Under the restriction of (30), the two inequalities in (31) are also not hard to be satisfied, if γ_f and γ_p are not too small at the same time. Based on the above general guidelines, more details for choosing γ_f and γ_p with other specific parameters can be discussed case by case. In the numerical experiment of the next section, the convergence and geometric convergence rate for multiple choices of γ_f and γ_p also show that it is not hard to choose these two parameters when K and ν are small. The theoretical analysis result in Theorem 2.1 is also consistent with the numerical result of Figure 6 with small K and ν in [8]. Hence the case of $\gamma_f > \gamma_p$, which is the target of this paper, is more useful than the case of $\gamma_f \le \gamma_p$ in practice.

3. Numerical experiment

In this section we present a numerical experiment to verify the presented theoretical convergence analysis. Consider the domain $\Omega = (0,1) \times (-0.25, 0.75)$, where the Darcy region $\Omega_D = (0,1) \times (0, 0.75)$, the Stokes region $\Omega_S = (0,1) \times (-0.25, 0)$ and the interface $\Gamma = [0,1] \times \{0\}$. Set $\alpha = 1$, $g = 1$ and $z = 0$. The boundary condition data functions and the source terms are chosen to satisfy the Stokes and Darcy equations by the following solution

$$\begin{cases} \phi_D = (2 - \pi sin(\pi x))\,(-y + cos(\pi(1-y)))\,, \\ \boldsymbol{u}_S = \left[x^2y^2 + e^{-y}, -\frac{2}{3}xy^3 + 2 - \pi sin(\pi x)\right], \\ p_S = -\,(2 - \pi sin(\pi x))\, cos(2\pi y), \end{cases}$$

which exactly satisfy the three interface conditions (3)–(4). Set $K = 10^{-6}$, $\nu = 10^{-6}$, $h = 1/32$, and $\gamma_f = 1.5$. Fig. 1 shows that the Robin–Robin algorithm converges when $\gamma_f > \gamma_p$ and the detailed data also verifies the geometric convergence rate $\sqrt{\frac{\gamma_p}{\gamma_f}}$. These results confirm Theorem 2.1.

4. Conclusions

For the case $\gamma_f > \gamma_p$, we analyze the convergence of the parallel Robin–Robin domain decomposition alongside a finite element discretization for solving the steady Stokes–Darcy system with BJ interface condition, based on the discrete harmonic and discrete Stokes extensions. This case is especially important for the parallel Robin–Robin domain decomposition method since the viscosity ν and hydraulic conductivity K are usually small in reality. The analysis result also provides a general guideline of choice on the relevant parameters to obtain the convergence and geometric convergence rate. The numerical results verify the theoretical conclusion.

Acknowledgment

The work was partially supported by National Science Foundation under Grant Number DMS-1722647.

References

[1] G.S. Beavers, D.D. Joseph, Boundary conditions at a naturally permeable wall, J. Fluid Mech. 30 (1) (1967) 197–207.
[2] Y. Cao, M. Gunzburger, X. Hu, F. Hua, X. Wang, W. Zhao, Finite element approximation for Stokes-Darcy flow with Beavers-Joseph interface conditions, SIAM J. Numer. Anal. 47 (6) (2010) 4239–4256.
[3] Y. Cao, M. Gunzburger, F. Hua, X. Wang, Coupled Stokes-Darcy model with Beavers-Joseph interface boundary condition, Commun. Math. Sci. 8 (1) (2010) 1–25.
[4] J. Hou, M. Qiu, X.-M. He, C. Guo, M. Wei, B. Bai, A dual-porosity-Stokes model and finite element method for coupling dual-porosity flow and free flow, SIAM J. Sci. Comput. 38 (5) (2016) B710–B739.
[5] W. Feng, X.-M. He, Z. Wang, X. Zhang, Non-iterative domain decomposition methods for a non-stationary Stokes-Darcy model with Beavers-Joseph interface condition, Appl. Math. Comput. 219 (2) (2012) 453–463.
[6] C. Qiu, X.-M. He, J. Li, Y. Lin, A domain decomposition method for the time-dependent Navier–Stokes-Darcy model with Beavers-Joseph interface condition and defective boundary condition, J. Comput. Phys. 411 (2020) #109400.
[7] W. Jäger, A. Mikelić, On the interface boundary condition of Beavers, Joseph, and Saffman, SIAM J. Appl. Math. 60 (4) (2000) 1111–1127.
[8] Y. Cao, M. Gunzburger, X. He, X. Wang, Robin-Robin domain decomposition methods for the steady-state Stokes-Darcy system with the Beavers-Joseph interface condition, Numer. Math. 117 (4) (2011) 601–629.
[9] W. Chen, M. Gunzburger, F. Hua, X. Wang, A parallel Robin-Robin domain decomposition method for the Stokes-Darcy system, SIAM J. Numer. Anal. 49 (3) (2011) 1064–1084.
[10] X.-M. He, J. Li, Y. Lin, J. Ming, A domain decomposition method for the steady-state Navier–Stokes-Darcy model with Beavers-Joseph interface condition, SIAM J. Sci. Comput. 37 (5) (2015) S264–S290.
[11] Y. Cao, M. Gunzburger, X.-M. He, X. Wang, Parallel, non-iterative, multi-physics domain decomposition methods for time-dependent Stokes-Darcy systems, Math. Comp. 83 (288) (2014) 1617–1644.
[12] M. Gunzburger, X.-M. He, B. Li, On Ritz projection and multi-step backward differentiation schemes in decoupling the Stokes-Darcy model, SIAM J. Numer. Anal. 56 (1) (2018) 397–427.
[13] R. Hoppe, P. Porta, Y. Vassilevski, Computational issues related to iterative coupling of subsurface and channel flows, Calcolo 44 (1) (2007) 1–20.
[14] A. Toselli, O. Widlund, Domain Decomposition Methods—Algorithms and Theory, in: Springer Series in Computational Mathematics, vol. 34, Springer-Verlag, Berlin, 2005.
[15] S.C. Brenner, L.R. Scott, The Mathematical Theory of Finite Element Methods, third ed., in: Texts in Applied Mathematics, vol. 15, Springer, New York, 2008.
[16] J.H. Bramble, J.E. Pasciak, A domain decomposition technique for Stokes problems, Appl. Numer. Math. 6 (4) (1990) 251–261.
[17] V. Girault, P.-A. Raviart, Finite Element Methods for Navier-Stokes Equations, in: Springer Series in Computational Mathematics, vol. 5, Springer-Verlag, Berlin, 1986, theory and algorithms.
[18] R.A. Adams, J.J.F. Fournier, Sobolev Spaces, second ed., in: Pure and Applied Mathematics (Amsterdam), vol. 140, Elsevier/Academic Press, Amsterdam, 2003.
[19] M. Discacciati, Domain Decomposition Methods for the Coupling of Surface and Groundwater Flows (Ph.D. thesis), Ecole Polytechnique Fédérale de Lausanne, Swizerland, 2004.